Tandem Measurements of Aerosol Properties—A Review of Mobility Techniques with Extensions

Park, K; Dutscher, D; Emery, M; Pagels, Joakim; Sakurai, H; Scheckman, J; Qian, S; Stolzenburg, MR; Wang, X; Yang, J; McMurry, PH

Published in:
Aerosol Science and Technology

DOI:
10.1080/02786820802339561

2008

Aerosol Science and Technology
Publication details, including instructions for authors and subscription information:
http://www.informaworld.com/smpp/title~content=t713656376

Tandem Measurements of Aerosol Properties—A Review of Mobility Techniques with Extensions

K. Park[a]; D. Dutcher[b]; M. Emery[b]; J. Pagels[c]; H. Sakurai[d]; J. Scheckman[b]; S. Qian[e]; M. R. Stolzenburg[f]; X. Wang[g]; J. Yang[b]; P. H. McMurry[b]
[a] Department of Environmental Science and Engineering, Gwuangju Institute of Science and Technology, Gwangju, Republic of Korea [b] Department of Mechanical Engineering, University of Minnesota, Minneapolis, Minnesota, USA [c] Ergonomics and Aerosol Technology, Lund University, Lund, Sweden [d] NMIJ/AIST, Tsukuba, Ibaraki, Japan [e] TSI Inc., Minneapolis, Minnesota, USA [f] Aerosol Dynamics, Inc., Berkeley, California, USA [g] TSI Inc., St. Paul, Minnesota, USA

First published on: 01 October 2008

To cite this Article Park, K. , Dutcher, D. , Emery, M. , Pagels, J. , Sakurai, H. , Scheckman, J. , Qian, S. , Stolzenburg, M. R. , Wang, X. , Yang, J. and McMurry, P. H.(2008) 'Tandem Measurements of Aerosol Properties—A Review of Mobility Techniques with Extensions', Aerosol Science and Technology, 42: 10, 801 — 816, First published on: 01 October 2008 (iFirst)
To link to this Article: DOI: 10.1080/02786820802339561
URL: http://dx.doi.org/10.1080/02786820802339561

Aerosol Science and Technology, 42:801–816, 2008

ISSN: 0278-6826 print / 1521-7388 online
DOI: 10.1080/02786820802339561

Tandem Measurements of Aerosol Properties—A Review of Mobility Techniques with Extensions

K. Park,[1] D. Dutcher,[2] M. Emery,[2] J. Pagels,[3] H. Sakurai,[4] J. Scheckman,[2] S. Qian,[5] M. R. Stolzenburg,[6] X. Wang,[7] J. Yang,[2] and P. H. McMurry[2]

[1]*Department of Environmental Science and Engineering, Gwuangju Institute of Science and Technology, Gwangju, Republic of Korea*
[2]*Department of Mechanical Engineering, University of Minnesota, Minneapolis, Minnesota, USA*
[3]*Ergonomics and Aerosol Technology, Lund University, Lund, Sweden*
[4]*NMIJ/AIST, Tsukuba, Ibaraki, Japan*
[5]*TSI Inc., Minneapolis, Minnesota, USA*
[6]*Aerosol Dynamics, Inc., Berkeley, California, USA*
[7]*TSI Inc., St. Paul, Minnesota, USA*

When multiple instruments are used in tandem it is possible to obtain more complete information on particle transport and physicochemical properties than can be obtained with a single instrument. This article discusses tandem measurements in which submicrometer particles classified according to electrical mobility are then characterized with one or more additional methods. Measurement combinations that are summarized here include mobility plus mass, aerodynamic (or vacuum aerodynamic) diameter, integrated or multiangle light scattering, composition by single particle mass spectrometry, electron microscopy, and so on. Such measurements enable intercomparisons of different measures of size including mobility diameter, optical size, aerodynamic diameter, volume (for agglomerates and nanowires), length (for nanowires), and mass, even for particles that are morphologically and chemically complex. In addition, the article summarizes the use of tandem techniques to measure various transport properties (e.g., dynamic shape factor, sedimentation speed, diffusion coefficient) and physicochemical properties (e.g., mixing state, shape, fractal dimension, density, vapor pressure, equilibrium water content, composition). In addition to providing an overview of such tandem measurements we describe previously unreported results from several novel tandem measurement methods.

Received 2 February 2008; accepted 11 July 2008.

The research described in this article was supported by NSF Grants ATM 0096555 and BES-0646507 to the University of Minnesota. DDD is funded by the Graduate Research for the Environment Fellowship, Global Change Education Program, Department of Energy. The final data analysis was partially supported by Eco Science-Technology Advancement Research Project by MOE, Korea Research Foundation Grant (KRF-2007-331-D00222), and Korea Science and Engineering Foundation (KOSEF) grant (No. R01-2007-000-10391-0).

Address correspondence to P. H. McMurry, University of Minnesoata, Department of Mechanical Engineering, Institute of Technology, 111 Church Street SE, Minneapolis MN 55455-0111, USA. E-mail: mcmurry@me.umn.edu

NOMENCLATURE*

a	radius of primary particle in an agglomerate
B	mechanical mobility
C_c	slip correction factor
c*	dimensionless drag force
c_m	aerosol mass concentration
D	diffusivity
$dc_m/d\log d_m$	aerosol mass distribution function
d_a	aerodynamic diameter
d_f	nanowire (nanotube) diameter
D_f	fractal dimension
d_m	mobility diameter
d_{pae}	projected area equivalent diameter
d_{ve}	volume equivalent diameter
e	elementary charge
F	aerodynamic drag force
k	Boltzmann constant
Kn	Knudsen number $= 2\lambda/d$
m	particle mass
n_p	number of elementary charges
T	temperature
v	particle volume
V	electrophoretic drift velocity
Z	electrical mobility
χ	dynamic shape factor
λ	mean free path of carrier gas
μ	viscosity of carrier gas
$\rho_{particle}$	inherent material density of particle $= m/v$
$\rho_{effective}$	effective density $= 6m/\pi d_m^3$
ρ_0	unit density (1 g/cm^3)

*The superscripts ^{atm} and ^{v} refer to properties measured at pressures of 1 atmosphere and 260 Pa, respectively.

INTRODUCTION

Fine and ultrafine particles in the atmosphere are of interest because of their effects on the earth's radiation budget (IPCC 2007), visibility impairment (NRC 1993), and human health (Oberdörster 2000; Peters et al. 1997). These effects depend on particle "size," morphology, and composition. It is now well established that different measurement methods provide different measures of particle size. For example, atmospheric particles of a given mobility size commonly have several different optical sizes (Covert et al. 1990; Dick and McMurry 2007; Dockery and Pope 1994; Heintzenberg et al. 2002; Heintzenberg et al. 2004; Hering and McMurry 1991; Naoe and Okada 2001; Okada and Heintzenberg 2003), masses (Geller et al. 2006; McMurry et al. 2002), and aerodynamic sizes (DeCarlo et al. 2005; McMurry et al. 2002), indicating that they are chemically and/or morphologically different. There is a need to understand the particle chemical and physical properties that determine these relationships. Recent work on tandem measurements of multiple particle properties has begun to provide such information.

Analytical chemists have used ion mobility spectrometers (IMS) in tandem with gas chromatographs (GC), liquid chromatographs (LC), and mass spectrometers (MS) to obtain information about structures of ion clusters and large molecules (Eiceman and Karpas 2005). For example, IMS-MS measurements have demonstrated that carbon cluster ions of a given mass have several discrete mobilities corresponding to different isomers (von Helden et al. 1991) and that the structure of complex molecules such as proteins changes with charge (Clemmer et al. 1995). De la Mora and coworkers have developed differential mobility analyzers (DMA) suitable for high resolution classification in the 1 nm range. They have carried out pioneering DMA-MS measurements that have provided new insights into mass-mobility relationships for ions and nanoparticles (Fernández de la Mora et al. 1998; Ude et al. 2006; Ude and Mora 2005) as well as DMA-impactor measurements aimed at measuring nanoparticle mass and impactor performance (Ude and de la Mora 2003). Similarly, Kaufman's gas-phase electrophoretic mobility molecular analyzer (GEMMA), which involves mobility classification with a DMA (Kaufman 1998), has been used with a mass spectrometer to determine molecular weight, size, and density of poly(amido-)amine (PAMAM) dendrimers (Müller et al. 2007).

Developments of tandem measurements in two areas are providing information on the properties of larger aerosol particles (10–1,000 nm) (McMurry 2000; McMurry et al. 2004). These include tandem measurements of mobility size followed by measurements of other properties including light scattering, mass, morphology and composition, and tandem measurements of particle aerodynamic size and/or optical properties followed by measurement of composition by mass spectroscopy (Canagaratna et al. 2007; DeCarlo et al. 2005; Nash et al. 2006; Noble and Prather 2000). This article focuses on tandem measurements for which particles are first classified according to mobility with conventional DMAs (Chen et al. 1998; Knutson and Whitby 1975; Liu and Pui 1974).

Table 1 lists instruments that we and others have applied in various combinations to mobility classified particles. Table 2 defines the acronyms found in Table 1 and elsewhere. A variant of this approach involves using a tandem differential mobility analyzer (TDMA) system (Rader and McMurry 1986) either separately or together with other measurement methods. TDMA measurements enable studies of various processes on particle properties. Processes that have been investigated with TDMAs include the condensation and evaporation of liquids, and chemical reactions. The concept behind tandem measurements discussed in this overview is illustrated in Figure 1. Particles separated according to mobility can be analyzed directly with another method to obtain information on the distribution of another property for those mobility-classified particles.

TABLE 1
Instrumentation

Instrument	Measured Property	Reference
DMA	$Z = neB = \frac{neC_c(d_{me})}{3\pi\mu d_{me}} = \frac{neC_c(d_{ve})}{3\pi\mu d_{ve}\chi}$	(Knutson and Whitby 1975; Liu and Pui 1974)
APM	m	(Ehara et al. 1996)
ATOFMS	d_a^v; single particle composition	(Gard et al. 1997)
CCN	Activation when exposed to slightly supersaturated water vapor	(Delene and Deshler 2000; Hudson 1989; Roberts and Nenes 2005)
MALS	Light scattering intensity vs. polar and azimuthal angles	(Dick and McMurry 2007; Dick et al. 1998; Wyatt et al. 1988)
Impactor: MOUDI, LPI	d_a^{atm}	(Hering et al. 1977; Hering and Friedlander 1979; Marple et al. 1991)
OPCs	Integrated light scattering intensity	(Cooke and Kerker 1975; Heyder and Gebhart 1979; Liu and Daum 2000; Szymanski and Liu 1986)
TEM	Morphology, D_f; v	(Park et al. 2004a, 2004b)

TABLE 2
List of acronyms

AMS:	Aerodyne Aerosol Mass Spectrometer
APM:	Aerosol Particle Mass Analyzer
ATOFMS:	Aerosol Time-of-Flight Mass Spectrometer
CCN:	Cloud Condensation Nucleus Concentration
DMA:	Differential Mobility Analyzer
LPI:	Low Pressure Impactor
MALS:	Multiangle Light Scattering
MOUDI:	Microorifice Uniform Deposit Impactor
NAA:	Neutron Activation Analysis
OPCs:	Optical Particle Counters
TDCIMS:	Thermal Desorption Chemical Ionization Mass Spectrometer
TDMA	Tandem Differential Mobility Analyzer
HTDMA:	Hygroscopicity Tandem Differential Mobility Analyzer
RTDMA:	Reaction Tandem Differential Mobility Analyzer
VDMA:	Volatility Tandem Differential Mobility Analyzer
TEM:	Transmission Electron Microscope

Alternatively, the mobility-classified particles can undergo processing and the mobility distributions of those processed particles can be measured in a TDMA system before other instruments are used to measure additional properties. A challenge of such work involves developing data inversion approaches that provide the most quantitative possible information on measured distributions (Cubison et al. 2005; Emery 2005; Stolzenburg and McMurry 1988).

Table 3 summarizes measurement approaches that have been used with DMAs in tandem with other instruments for measuring various transport properties of submicrometer particles. Because electrical mobility and diffusivity both vary in proportion to mechanical mobility, diffusivity can be determined directly from mobility measurements. By adding a measurement of mass with the Aerosol Particle Mass analyzer (APM) (Ehara et al. 1996), it is possible to determine the sedimentation speed and aerodynamic diameter. Dynamic shape factors can be determined by using a Transmission Electron Microscope (TEM) to obtain estimates of the volume of irregularly shaped particles.

The preferential electrostatic orientation of irregularly shaped particles during electrical mobility classification can affect mobility classification if fields are sufficiently high or particles are sufficiently long. For example, it has been shown experimentally that large fibers (>0.1 μm) become aligned at field strengths of <1 kV/cm (Lilienfeld 1985), which are often exceeded in DMAs, and chain agglomerates formed from ~100 nm PSL spheres can align parallel to the electric field as they are classified by DMAs, leading to lower drag and higher mobilities than would occur for random orientations (Kousaka et al. 1996; Zelenyuk and Imre 200). The tendency of nanowires to align has also been studied in detail (Kim et al. 2007; Kim and Zachariah 2005, 2006). These studies showed that for fields up to 1 kV/cm, nanowires ($d_f = 15\ nm$) with aspect ratios less than 30 rotate freely due to Brownian rotation while those with aspect ratios exceeding 30 align with the field. The extent to which nonspherical particles orient may have a significant impact on values of D, v_s, d_a^v, d_a^{atm}, and χ that are determined from the tandem measurements summarized in Table 3.

Chan and Dahneke (1981) reported Monte Carlo simulations of drag for chain agglomerates in the free molecular regime assuming hard sphere collisions. The Basic Chain Unit (BCU) used in their calculations consisted of two hemispheres joined at their poles, and they reported results for the dimensionless drag, defined as (Chan and Dahneke 1981):

$$c^* = \frac{FKn}{\mu a V}. \quad [1]$$

In the limit of low transport speeds, the dimensionless drag on BCU traveling with axes parallel to the direction of motion was

TABLE 3
Measurements of transport properties

Transport Property	Instruments	Reference
Electrical Mobility: $Z = n_p eB$	DMA	(Knutson and Whitby 1975; Liu and Pui 1974)
Diffusivity: $D = kTB$	DMA	(Hinds 1999)
Sedimentation Speed: $v_s = mgB$	DMA + APM	(Hinds 1999)
Dynamic Shape Factor: $\chi = \frac{d_m}{d_{ve}} \frac{C_c(d_{ve})}{C_c(d_m)}$	DMA + TEM	(Kasper 1982; Park et al. 2004c)
Aerodynamic Diameter: $(d_a^{atm})^2 C_c(d_a^{atm}) = \frac{1}{\chi^{atm}} \frac{\rho_{particle}}{\rho_0} d_{ve}^2 C(d_{ve}) = \frac{\rho_{effective}}{\rho_0} d_m^2 C(d_m)$	DMA + APM	(McMurry et al. 2002); Figure 2
Vacuum aerodynamic diameter vs. mobility diameter $d_a^v = \frac{1}{\chi^v} \frac{\rho_{particle}}{\rho_0} d_{ve}$; $d_{ve}^2 C(d_{ve}) = \frac{6m\chi^{atm}}{\pi \rho_{particle} d_m} C(d_m)$	DMA + AMS DMA + ATOFMS	Figure 2

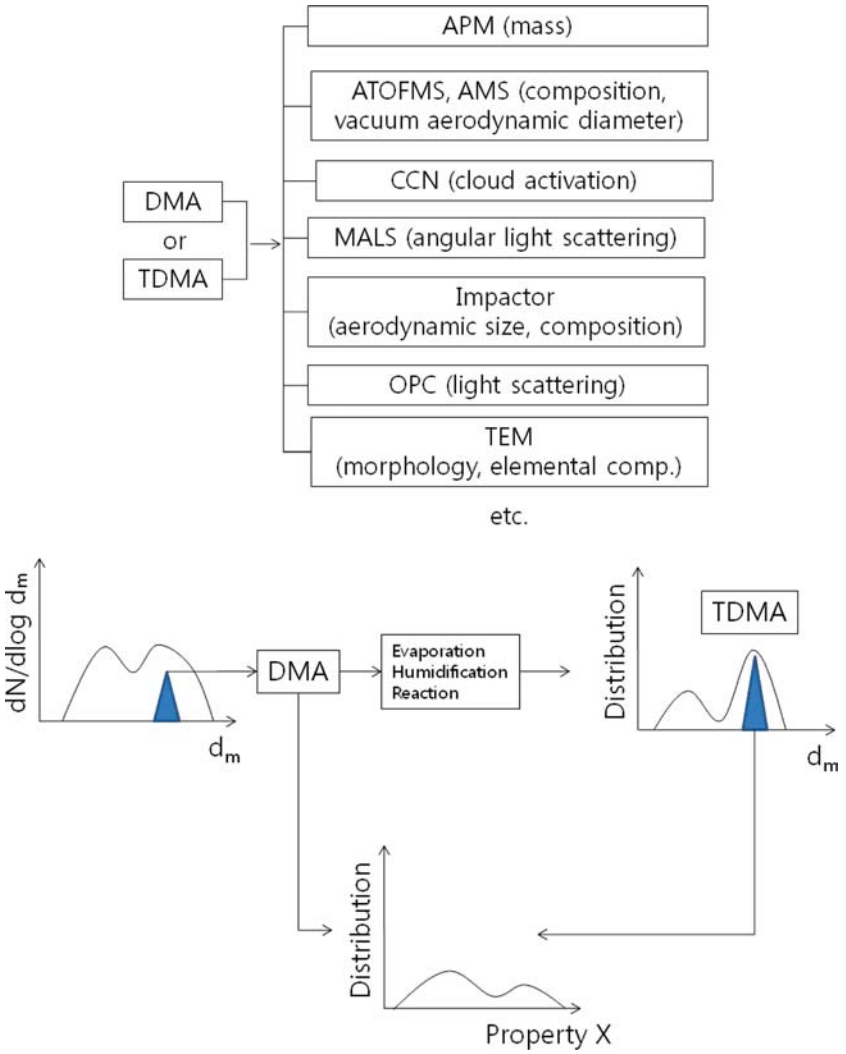

FIG. 1. Schematic of aerosol tandem measurements discussed in this article. Particles of a given mobility diameter are selected by a DMA from the sampled aerosol. Further information about aerosol physicochemical properties is obtained one or more additional measurement methods in series. An alternative involves using a TDMA to processes the aerosol prior to measuring additional properties.

equal to 4.59 and 6.77, respectively, for specular and diffuse reflections. For BCU moving with their axis perpendicular to the direction of motion, these values were 9.10 and 11.52. Corresponding values for randomly oriented BCU were found to be 6.85 and 9.34. It is known that collisions of molecules and ions are elastic, so for such collisions the specular results apply. Collisions of gas molecules with particles with mass diameters larger than ~2 nm, however, are inelastic (Tammet 1995), and the drag should be closer to (but still less than) the value for diffuse reflections (Li and Wang 2003a, 2003b). For spherical particles, empirical observations have shown that the dimensionless drag equals 5.77, corresponding to collisions that are approximately 10% specular and 90% diffuse (Li and Wang 2003a). For large chain agglomerate particles, such as would be produced in a combustion process, the overall orientations of pairs of primary particles during mobility classification in a DMA would likely be nearly random. However, if the agglomerate is longer along a particular axis, dipole interactions may cause it to align with the field in analogy to the previously mentioned observations for fibers. This may affect its mobility, and therefore the value of the dynamic shape factor determined from the mobility. Accordingly, care should be taken when using dynamic shape factors determined from measurements of electrical mobility when calculating values of diffusion coefficient or sedimentation speed, since particles may not align themselves in the same manner during such transport.

Table 4 summarizes some particle physical/chemical properties that have been measured using methods that involve preselecting particles with a DMA. In some cases these measurements have been carried out on atmospheric aerosols, while in other cases they were done on engine exhaust or well-characterized laboratory aerosols. Such measurements enable

TABLE 4
Measurements of particle physical/Chemical properties: DMA systems

Properties	Instruments	References
d_{pae} for agglomerates or nanowires	DMA	(Jung et al. 2004; Kim and Zachariah 2005; Park et al. 2004c; Rogak and Flagan 1993)
v or d_{ve} for agglomerates	DMA + TEM	(Lall and Friedlander 2006; Lall et al. 2008; Lall et al. 2006)
Length of Nanowires (Nanotubes)	DMA + TEM	(Kim et al. 2007; Kim and Zachariah 2005, 2006)
Bright/dark particle ratio & mixing state; d_m vs. optical size; water uptake	DMA + OPC	(Heintzenberg et al. 2002; Hering and McMurry 1991; Covert et al. 1990) (Sorooshian et al. 2008) Figure 3 Figure 4
Mixing state & morphology	DMA + OPC + TEM (OPC & TEM in parallel)	(Heintzenberg et al. 2004; Okada and Heintzenberg 2003)
n	DMA + MALS	(Dick and McMurry 2007)
Shape (spherical vs. nonspherical)	DMA + MALS	(Dick et al. 1998; Sachweh et al. 1995)
$\rho_{effective}$; d_m vs. m; D_f; morphology	DMA + APM DMA + Impactor DMA + TEM DMA + Mass Spectrometer Ion Mobility Spectrometer (IMS) + Mass Spectrometer	(de la Mora et al. 2003; Fernández de la Mora et al. 1998; Geller et al. 2006; Hering and Stolzenburg 1995; Kelly and McMurry 1992; Maricq and Xu 2004; McMurry et al. 2002; Olfert et al. 2007; Park et al. 2003a; Skillas et al. 1998; Slowik et al. 2004; Stein et al. 1994; Wyttenbach and Bowers 2007); Figure 5
$\rho_{particle}$	DMA + APM + TEM	(Park et al. 2004c; Park et al. 2004d)
$dc_m/d\log d_m$; c_m	DMA (SMPS) + APM	(Park et al. 2003b)
Elemental composition of ultrafine particles	DMA + NAA	(Neville et al. 1983)
Nanoparticle composition	DMA + TDCIMS	(Smith et al. 2008; Smith et al. 2005; Smith et al. 2004; Voisin et al. 2003)
Composition of individual mobility-classified particles	DMA + APM + ATOFMS (APM & ATOFMS in parallel)	Figure 6 Figure 7
Size-dependent cloud activation efficiencies	DMA + CCN	(Bilde and Svenningsson 2004; Corrigan and Novakov 1999; Cruz and Pandis 1997; Petters et al. 2007; Bilde and Svenningsson 2004; Corrigan and Novakov 1999; Cruz and Pandis 1997; Petters et al. 2007)

intercomparisons of different measures of size which can be helpful when merging data obtained using different measurement principles into a single, self-consistent measurement of size distribution. The measurements that are summarized in Table 4 include those that determine relationships between mobility diameter and light scattering intensity, mobility diameter and mass, mobility diameter and agglomerate or nanowire volume, and mobility diameter and aerodynamic (or vacuum aerodynamic) diameter. Such measurements can also be used to provide information on mixing state (mobility size vs. relative proportions of "bright" and "dark" particles; mobility size vs. categories of particles sorted according to composition; mobility size vs. the proportions of spherical and nonspherical particles; mobility size vs. the proportion of "low" and "high" mass

TABLE 5
Measurements of particle physical/Chemical Properties: TDMA systems

Properties	Instruments	References
Water uptake; mixing state	HTDMA	(Liu et al. 1978; McMurry and Stolzenburg 1989; Swietlicki et al. 2008)
Vapor pressure/volatility; mixing state	VTDMA	(Orsini et al. 1999; Philippin et al. 2004; Rader et al. 1987; Riipinen et al. 2007; Sakurai et al. 2003b; Tao and McMurry 1989; Villani et al. 2007)
Reactivity	RTDMA	(Gupta et al. 1995; Holm and Roberts 2007; Liao et al. 2006; Liao and Roberts 2006; McMurry et al. 1983; Zhang et al. 2008a)
Sintering or fusion of agglomerates	TDMA	(Cho et al. 2007; Nakaso et al. 2002)
Morphology & elemental composition-dependent water uptake	HTDMA + TEM	(McMurry et al. 1996)
Volatile mass fraction vs. T	VTDMA + APM	(Sakurai et al. 2003a)
Effective density vs. RH	HTDMA + APM	(Zhang et al. 2008b); Figure 8
Density vs. extent of volatilization; Density of evaporated mass	VTDMA + APM	Discussion
Dependence of composition on volatilization	VTDMA + ATOFMS	Figures 9 and 10
Cloud Activation of Coated Particles	RTDMA + CCN	(Abbatt et al. 2005; Cruz and Pandis 1998)

particles, etc.) Also noteworthy is the use of an APM to measure the mass of mobility-classified particles in an SMPS system: such measurements enable first-principles, in-situ measurements of mass distributions and mass concentrations of particles smaller than about 0.5 μm mobility diameter, thereby avoiding the positive and negative artifacts that are inherent to filter sampling.

Table 5 summarizes particle physical/chemical properties that have been measured using methods that involve TDMA systems. TDMA systems have been employed to study the effects of evaporation (VTDMA), humidification (HTDMA), and chemical reaction (RTDMA) on particle properties. It is also possible to use TDMAs in concert with other measurement systems, as summarized in Table 5 and illustrated in Figure 1. For example, the use of an APM downstream of a TDMA enables direct measurements of mass changes associated with conditioning. Such measurements can be especially informative for nonspherical particles, such as chain agglomerates, where conditioning may cause mobility to change as a result of changes in both structure and mass. For example, it has been observed that when vapor condenses on agglomerates they can collapse to more compact forms, causing their mobility size to decrease (Weingartner et al. 1997; Zhang et al. 2008b). The APM can quantify the amount of mass that condensed, thereby enabling quantitative observations on the relationship between the mass of liquid added and changes in mobility due to structuring. It is likely that such processes affect the properties of agglomerate particles as they undergo processing in the atmosphere. Similarly, when chemically complex spherical particles undergo volatilization, a distillation process would be expected, whereby the more volatile species would be lost first. By combining measurements of mobility size and mass, it is possible to track the density of the particle as it evaporates. Single particle mass spectrometers, such as the Aerosol Time of Flight Mass Spectrometer (ATOFMS), can be used to directly track changes in composition during such processing. The references and tandem methods given in Tables 4 and 5 are illustrative and are by no means comprehensive. For example, the recent review article on HTDMA measurements of water uptake by atmospheric aerosols cited more than 140 papers on this topic alone (Swietlicki et al. 2008).

Tandem measurements that have been reported in the literature for measuring particle properties were briefly summarized above and are discussed in detail in the references cited in Tables 3–5. In the remainder of the article we discuss illustrative results of several new tandem measurements. The examples that are discussed were chosen because they illustrate new types of information that can be measured using tandem methods, because they synthesize diverse results of tandem measurements, or because they illustrate unexpected limitations that we encountered when attempting new tandem measurements.

New Tandem Measurements

The new results that will be discussed in this section are identified in Tables 4 and 5. These measurements include studies on well-defined laboratory aerosols, particles produced in a propane flame burner, diesel exhaust particles, and atmospheric aerosols. The atmospheric measurements were carried out

during the EPA supersite study in St. Louis (Pandis et al. 2005; Sioutas et al. 2004; Stanier and Solomon 2006) and at the Jefferson St. site in Atlanta during the ANARChE study (McMurry and Eisele 2005).

Mobility Diameter Versus Aerodynamic Diameter

Figures 2–5 show new results that contrast different measurements of particle size. Figure 2 shows the relationship between vacuum aerodynamic diameter measured at 260 Pa with the ATOFMS and mobility diameter. Data are shown for polystyrene latex (PSL) spheres and for agglomerate soot particles produced in a propane diffusion flame burner. Also shown on this figure are similar results for flame soot obtained using the Aerodyne AMS (Slowik et al. 2004). In both the AMS and the ATOFMS, the vacuum aerodynamic size is determined from the terminal speeds that particles achieve when accelerated through a nozzle at about 260 Pa (2 torr) into a chamber at a much lower pressure. The ATOFMS uses light scattering to determine the time-of-flight between two lasers located a known distance apart along the particle's flight trajectory while the AMS uses the time required for particles to travel from a particle beam chopper to

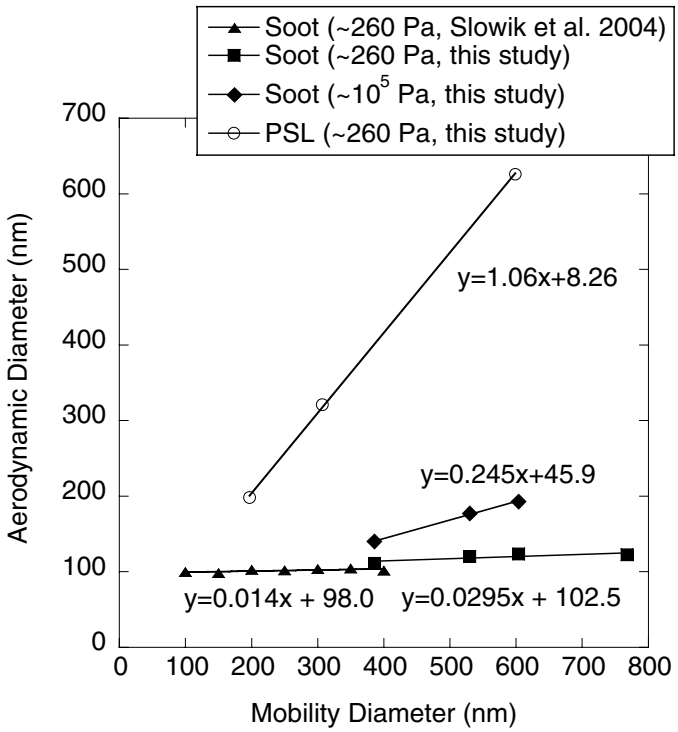

FIG. 2. DMA-ATOFMS measurements of vacuum aerodynamic diameter d_a^v vs. mobility diameter d_m for polystyrene latex (PSL) spheres and for flame soot agglomerates. The value of the slope of the linear relationship between d_a^v and d_m for the spherical PSL particles (1.06) is close to the PSL density (1.054 g cm^{-3}), as expected from theory (DeCarlo et al. 2005). Also shown are data for flame soot obtained using a DMA and an Aerodyne AMS (Slowik et al. 2004) (the "type I" particles in that study). The ATOFMS data shown here apply to lean combustion conditions. Also shown are calculated aerodynamic diameters at atmospheric pressure for the soot measured in this study.

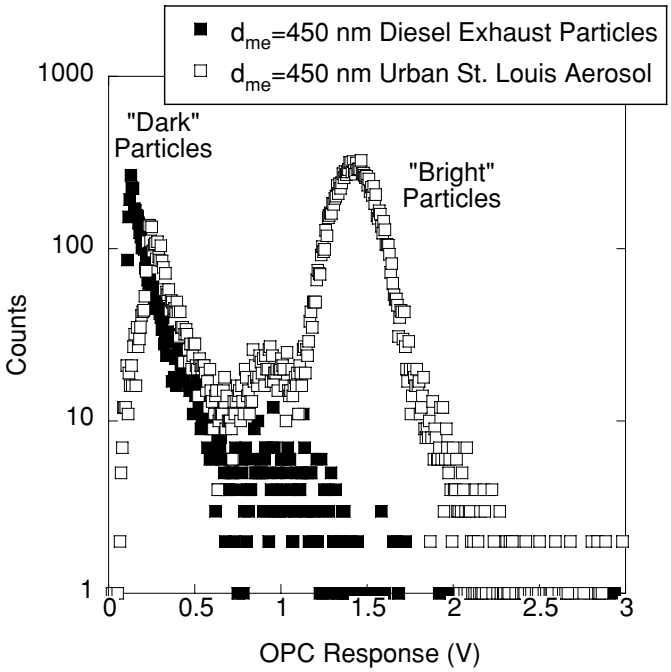

FIG. 3. DMA-OPC measurements of count frequency vs. light scattering intensity for 450 nm mobility diameter particles. Data are shown for measurements in urban St. Louis (July 8 and 9, 2001) and for laboratory measurements of diesel exhaust aerosol. Note that the optical signature of the diesel exhaust particles is similar to that for the "dark" particles (i.e., those that scattered relatively little light and therefore produced a small voltage pulse) that were observed in St. Louis. On these two days, most of the particles in St. Louis were "bright," and likely consisted of sulfate/organic mixtures.

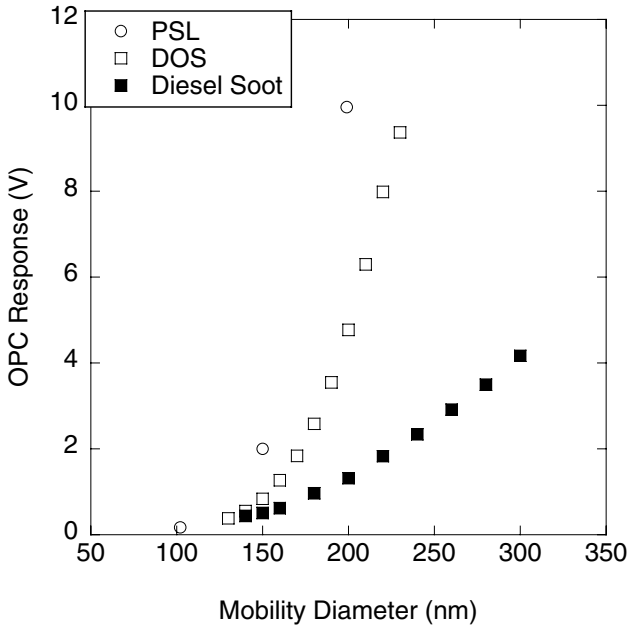

FIG. 4. DMA-OPC measurements of measured light scattering intensity vs. mobility diameter for polystyrene spheres (PSL), dioctyl sebacate (DOS) oil droplets, and diesel exhaust soot. OPC measurements were done using a PMS Lasair 1002. The diesel soot was measured in the exhaust of a John Deere 4045 engine operating with 400 ppm sulfur fuel at 50% load (Wang 2002).

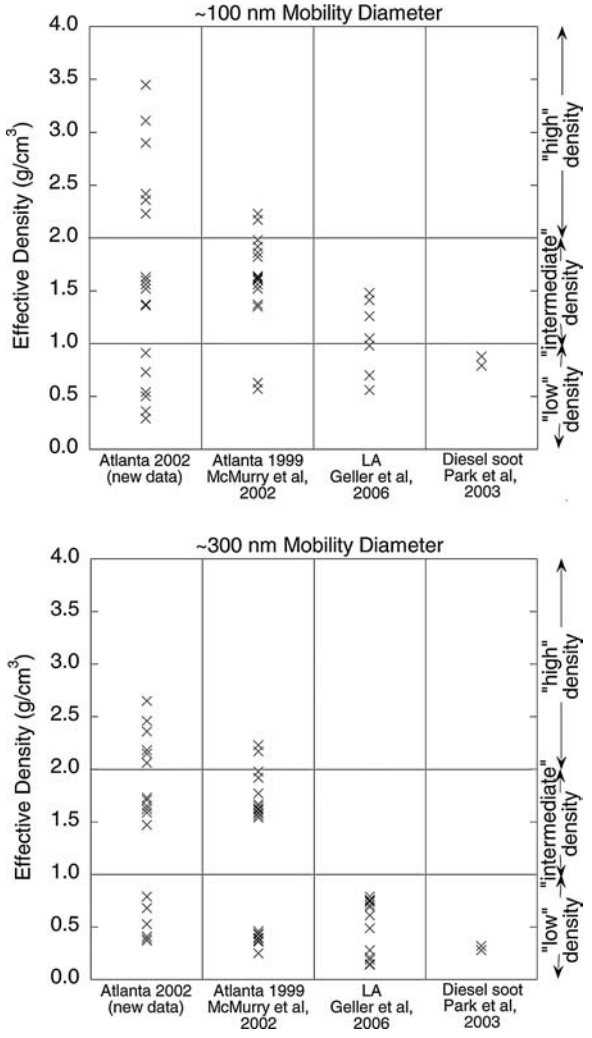

FIG. 5. DMA-APM measurements of effective density for particles with nominal mobility size of 100 and 300 nm. The data from the 2002 study in Atlanta are compared with previous measurements in Atlanta and Los Angeles using the same measurement method. Laboratory measurements for diesel exhaust particles are also shown. We have categorized the effective densities as "low" (<1 g/cm^3), "intermediate" (1.0–2.0 g/cm^3), and "high" (>2.0 g/cm^3).

the chemical sensor. Because the AMS does not require optical detection, its measurements of vacuum aerodynamic diameter extend to smaller sizes. These results show that the vacuum aerodynamic sizes of PSL spheres measured by the ATOFMS are in excellent agreement with the expected values. However, for the soot agglomerates the vacuum aerodynamic sizes measured by both the AMS and ATOFMS are nearly independent of mobility size over the 100–800 nm size range investigated. This is because the terminal velocity that determines these aerodynamic sizes depends on the particle acceleration (i.e., aerodynamic drag force per unit mass) within the jet. In the limiting case that primary particles in an agglomerate were not shielded by their neighbors, each individual primary particle would experience the same force and the agglomerate's terminal velocity would equal that for an isolated single primary particle independent of the agglomerate's size. The sizes of the primary soot particles in our measurements were in the 30–35 nm range, so this limiting case argument does not hold exactly for these agglomerates. However, the observation that the vacuum aerodynamic size is nearly independent of mobility size (which, we know, is a strong function of the agglomerate mass) shows clearly that the acceleration force per unit mass is nearly independent of the agglomerate size. Also shown in Figure 2 are aerodynamic diameters at atmospheric pressure calculated from mass and mobility size using the equation given in Table 3. The aerodynamic size at atmospheric pressure increases from 140 nm to 193 nm as mobility sizes increase from 386 to 768 nm. This 38% increase is significantly greater than the 11% increase observed for the vacuum aerodynamic diameter, which increased from 111 to 123 nm as mobility diameter increased from 386 to 768 nm, but still not sufficient for enabling clear separations using aerodynamic classification. Using Monte-Carlo calculations, Barone et al. (2006) also showed that the aerodynamic diameter of the agglomerate is independent of the number of primary particles that compose an agglomerate (i.e., agglomerate mass) (Barone et al. 2006).

The results shown in Figure 2 have important implications for the characterization of atmospheric aerosols. The aerodynamic sizes of these agglomerates, whether measured at low or atmospheric pressure, provide virtually no information about particle mass or diffusivity (which varies in proportion to mobility). Aerodynamic classifiers such as impactors are often used to sample atmospheric particles, and aerodynamic size is also used in size-selective inlets. In a properly functioning impactor, for example, virtually all of the soot should be collected on one or at most two stages even though the masses of individual agglomerate particles could vary over more than an order of magnitude. Since lung deposition of ultrafine particles (<100 nm) is more likely to be determined by particle diffusivity than inertia, it follows that inertial classifiers provide little useful information on the health effects of such particles. On the other hand, the clear separation of mobility-classified agglomerates from more compact particles in instruments such as the Aerodyne AMS is a powerful tool for identifying particles according to type.

Mobility Diameter Versus Optical Diameter

Figure 3 shows the results of light scattering measurements carried out with a PMS Lasair Model 1002 optical particle counter (OPC) on mobility-classified 450 nm particles in St. Louis. These pulse height distributions were obtained by using a multichannel analyzer (MCA) to categorize pulse heights produced by the OPC's photodetector. Our measurement protocol in St. Louis involved sampling mobility-classified 450 nm particles with the OPC for the first ten minutes of every hour during the 2-year measurement campaign. Illustrative results for the St. Louis aerosol are compared with pulse height distributions from laboratory measurements of diesel exhaust particles. A John Deere 4050 engine operating at 50% load with 400 ppm S fuel was

used in this study. Note that the ambient aerosols produce two distinct peaks, as has been observed previously (Covert et al. 1990; Heintzenberg et al. 2002; Heintzenberg et al. 2004; Hering and McMurry 1991; Okada and Heintzenberg 2003). The amount of light scattered by the urban St. Louis particles in the smaller voltage peak is similar to that scattered by the diesel exhaust particles. This is consistent with the hypothesis that the "dark" particles in St. Louis are primary soot agglomerates. The "bright" particles likely consist of liquid spheres that consist primarily of sulfates and organics (Dick and McMurry 2007; Dick et al. 2000; Okada and Heintzenberg 2003).

The response of the PMS Lasair 1002 OPC to PSL and dioctyl sebacate (DOS) spheres and to mobility-classified diesel exhaust particles is compared in Figure 4. Note that for particles of a given mobility size, the PSL systematically scatters more light than the DOS. This is because PSL has a higher refractive index than DOS. Also, PSL and DOS both scatter considerably more light than diesel exhaust particles of the same mobility size. In principle, calibrations such as these can be used to establish the relationship between the light scattering response of OPCs to particles of known mobility size. Such calibrations can be done for particles of arbitrary shape and composition, thereby enabling the direct measurement of mobility distributions with OPCs. However, as was shown for the externally-mixed St. Louis aerosol in Figure 3, there may not be a unique relationship between mobility size and optical response. In such a case, determining the relationship between mobility size and OPC response would require routine parallel measurements of the proportions of each particle type. The fact that a large fraction of the submicrometer particles scatter too little light to be detected by an OPC would also complicate such measurements.

Mass-Mobility Relationships (Effective Density)

Figure 5 shows effective densities of nominally 100 nm and 300 nm mobility diameter urban Atlanta particles measured using the DMA-APM technique. For comparison, data for urban Los Angeles particles (Geller et al. 2006) and diesel exhaust particles (Park et al. 2003a) measured using the same method are also shown. These effective densities are defined as mass measured by the APM divided by volume calculated assuming that the mobility-classified particles are spheres. If the particles are spheres, then the effective density equals the true density. If particles are not spherical, then the calculated volume exceeds the true volume and the effective density is less than the true density. Because two or three distinct masses are typically detected for particles of a given mobility size, these data provide information both on mixing characteristics and on the relationship between mobility size and mass. The "low density" particles likely consist primarily of agglomerate soot, while the intermediate density particles likely consist of primarily organic/sulfate mixtures. The densities of particles measured in Atlanta during 2002 extended to values that were higher than were observed previously, and we are not sure about the composition of those particles, but the results of the two Atlanta studies and the Los Angeles study are otherwise qualitatively consistent. We have carried out calculations to confirm that the high density particles are not an artifact of multiple charging (McMurry et al. 2002). The effective densities of the 100 nm particles in all three urban studies and the effective density of the 300 nm particles in Los Angeles extended to values that were lower than were measured for diesel soot in the laboratory. This could reflect differences in emissions characteristics of vehicle fleets when compared to the single engine used in the laboratory study. It is also possible that the particles with the lowest effective densities are emitted by a different type of source.

Mobility-Mass-Chemical Composition

Figure 6 shows the response of an ATOFMS when sampling 500 nm mobility diameter particles from the exhaust of a Caterpillar C-12 heavy duty diesel engine operating at 20% load and 1200 rpm. As shown in Figure 6a, these particles are cleanly separated into two groups, one with vacuum aerodynamic diameter peaking at 108 nm and the other with vacuum aerodynamic diameter peaking at 580 nm. The compositions of these two categories of particles are distinctly different. Those with the small vacuum aerodynamic sizes contain primarily soot, while those with the larger vacuum aerodynamic diameters contain species associated with lubricating oil. Thus, by using an ATOFMS to sample mobility-classified particles, it is possible to learn about composition-dependent mixing characteristics.

Figure 7 shows measurements obtained using the ATOFMS to sample particles of 300 nm mobility size that had been preclassified by a DMA and an APM. Measurements were done using particles consisting of mixtures of sulfuric acid and ammonium sulfate in molar ratios ranging from 0:1 to 1:0. As the particles became more acidic, the ATOFMS spectra show peaks at masses +59 and +99, which are not associated with either sulfuric acid or ammonium sulfate. Furthermore, the intensities of these peaks varied approximately linearly with the mole fraction of sulfuric acid in the sampled particles. Separate measurements on particles made by atomizing the ferrofluid used in the APM rotating seals show that those masses are associated with that fluid. We hypothesize based on the ATOFMS spectra that the contaminant species is a semi-volatile secondary amine species; this class of species is often used in ferrofluids as an anti-oxidant. Because the intensity of this artifact signal is so strong, we have been unable to carry out ATOFMS measurements of composition for atmospheric particles that were first classified by mass with the APM.

Mobility-Hygroscopicity (or Volatility)-Mass-Chemical Composition

Figure 8 shows in situ measurements of particle density for urban Atlanta aerosols as a function of relative humidity. These measurements were obtained using a HTDMA to measure the dependence of relative humidity on size, and an APM to measure

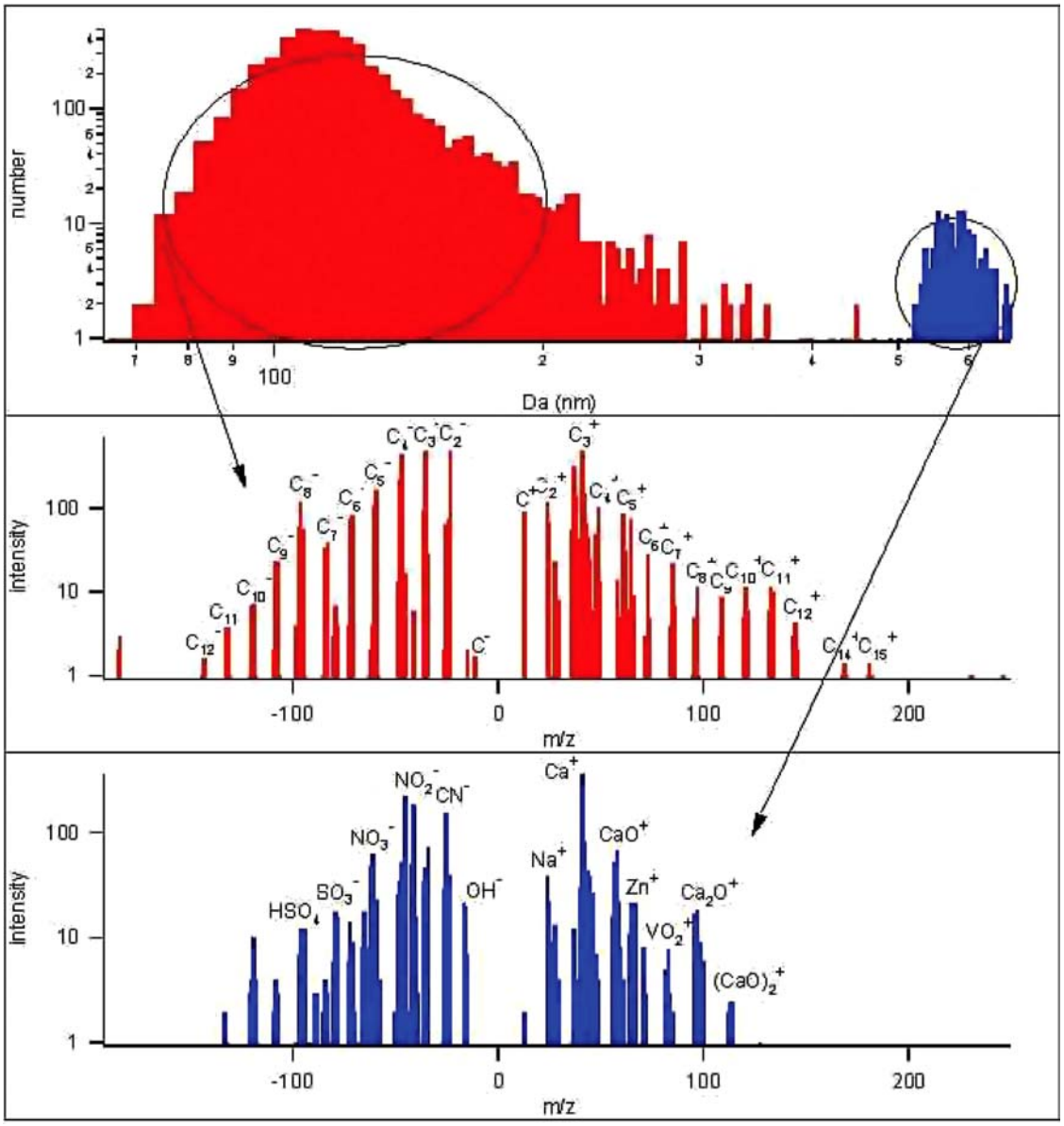

FIG. 6. DMA-ATOFMS measurements of 500 nm mobility diameter particles from the exhaust of a Catepillar C-12 heavy duty diesel engine. Note that when classified according to vacuum aerodynamic diameter, d_a^v, these particles separate cleanly into two groups with distinctly different compositions. Those with smaller d_a^v consist primarily of carbon soot. Those with larger d_a^v consist primarily of sulfates and metals.

the corresponding mass of particles after they had absorbed water. The densities shown in this figure apply only to the "more hygroscopic" particle fraction (McMurry and Stolzenburg 1989) and were calculated assuming that particles were spherical, which should be reasonable given that their densities exceed 1 g/cm^3 (so they probably are not agglomerates) and that they contain significant amounts of water. The densities decreased from 1.5–1.7 g/cm^3 at low RH to around 1.2–1.4 g/cm^3 at 80% RH. To our knowledge, these are the first direct measurements of the density of hygroscopic atmospheric particles.

Since we are able to measure the mass of particles after and before water uptake using the HTDMA-APM technique, it was also possible to estimate the water mass fraction. If the water mass in particles classified by DMA1 at ~7% RH is negligible, this would provide a reasonable estimate of the water mass in particles at 80% RH. The mass fraction of water for 100 nm "more hygroscopic" particles varied from 45–48% at 80% RH, which is lower than the mass fraction of water that is thermodynamically predicted for pure ammonium sulfate particles (56%) or pure sulfuric acid (74%) at 80% RH. For 300 nm particles, the mass fraction of water at 80% RH was 61–67%, which is higher than expected for pure ammonium sulfate particles but smaller than for pure sulfuric acid particles. It is likely that organic compounds are responsible for the absorption of some of this

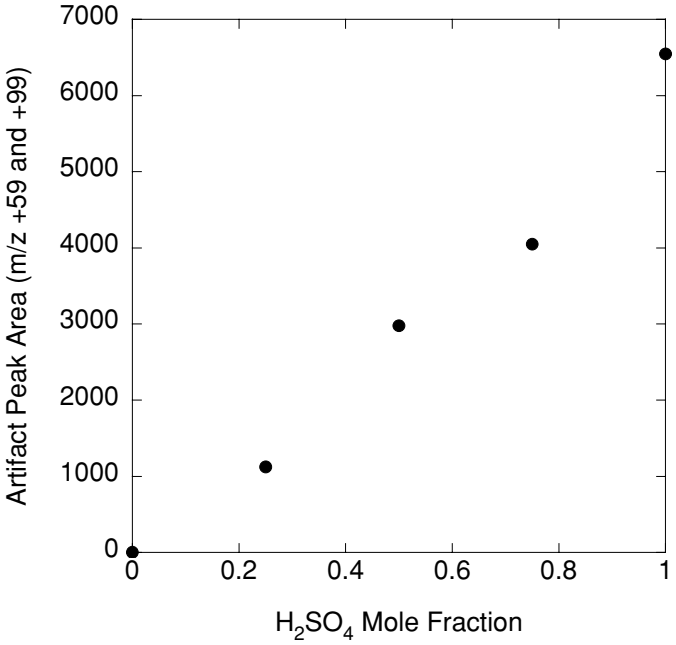

FIG. 7. DMA-APM-ATOFMS measurements of artifacts that occur when particles consisting of sulfuric acid/ammonium sulfate internal mixtures flow through the APM. Plotted is the sum of mass 59 plus 99 peaks vs. the sulfuric acid mole fraction in laboratory calibration particles of 300 nm mobility size. Separate measurements on atomized ferrofluid used in the APM rotating seals show that those peaks are associated with this ferrofluid. The artifact arises when a basic gas, volatilized from the ferrofluid, is absorbed by the acidic particles.

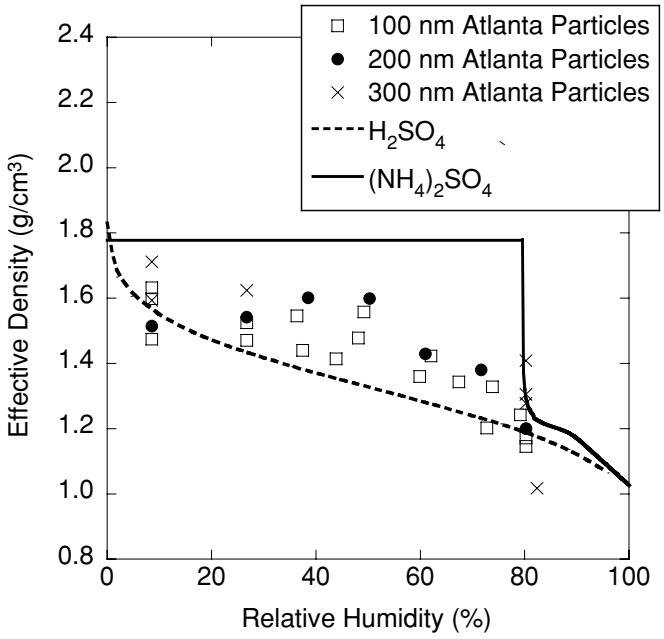

FIG. 8. HTDMA-APM measurements of effective densities of atmospheric particles measured in urban Atlanta (2002) along with thermodynamic predictions for pure ammonium sulfate and sulfuric acid particles as a function of relative humidity.

water (Dick et al. 2000; Saxena and Hildemann 1996; Saxena and Hildemann 1997). Atmospheric particles also likely contain nonhygroscopic species, such as soot, metal oxides, or hydrocarbons, that do not absorb water. The presence of such species would reduce the mass fractions of water. On the other hand, the absorption of water by very hygroscopic inorganic species such as NaCl and KCl, or into voids or pores in particles would cause water mass fractions to exceed values calculated for sulfates or sulfuric acid. Measurements of this type should eventually enable a quantitative understanding of the relationship between the amount of water in multicomponent atmospheric particles and their composition. Again, we believe these are the first direct in situ measurements of water mass in atmospheric particles.

Density measurements of "less hygroscopic" particles demonstrated that particles having effective densities of 0.21–0.87 g/cm^3 at 80% RH were among the "less hygroscopic" particles. The mass fraction of water for 100 nm "less hygroscopic" particles, which grew by only 3% in mobility size when humidified to 80% RH, was about 5%. There is no obvious relationship between the observed change in mobility size and the change in mass associated with water uptake for these particles, which are presumably agglomerates.

Several VTDMA measurements were carried out in Atlanta to study the effect of evaporation on particle density and composition. These measurements involved classifying particles of 100 or 300 nm with DMA1, heating them to a known temperature in the 25 to 300°C range for a known period of time (~200 ms), determining the resulting mobility size with DMA2, and measuring the mass (APM) or composition (ATOFMS) of the DMA2-classified particles. When heated, mobility-classified particles typically separated into two clearly distinct mobility sizes for heater temperatures above about 150°C; similar results have also been observed by others (Philippin et al. 2004; Villani et al. 2007). Above this temperature the "less volatile" particles reached an asymptotic size and the decrease in mobility size for these particles ranged from 0 to 5 nm, while the "more volatile" particles continued to evaporate as temperature increased. Tandem measurements of mass with the APM and composition with the ATOFMS provided information on the effect of heating on effective density and composition. This approach also permits measuring the chemical makeup of particles that were segregated according to volatility.

By dividing the decrease in mass by the decrease in volume (assuming that particles were spherical), the effective density of evaporated mass can be found from VTDMA-APM measurements. We carried out exploratory VTDMA-APM measurements on the "more volatile" particle fraction during the 2002 Atlanta study. We reasoned that, due to their high abundances and their effective densities in the 1.5 g/cm^3 range, these particles were probably liquid spheres. If so, the measured effective densities would equal true material densities. We found that for 300 nm particles, the effective density of the evaporated mass was 1.89 g/cm^3, which is close to the density of ammonium sulfate (1.78 g/cm^3) or sulfuric acid (1.84 g/cm^3). The effective

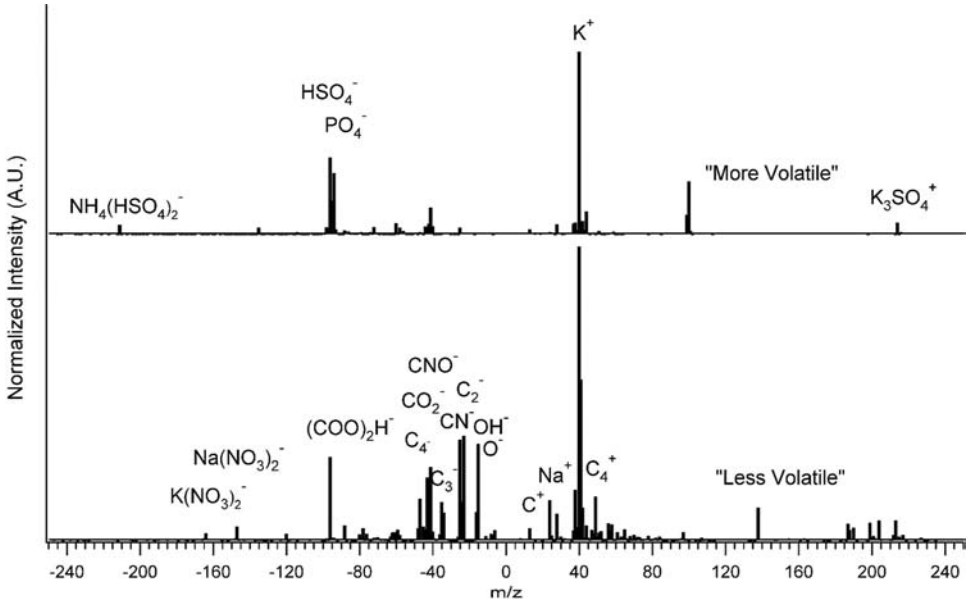

FIG. 9. VTDMA-ATOFMS measurements of comparison of averaged (a) positive and (b) negative ion mass spectra for "more volatile" and "less volatile" 300 nm mobility diameter particles in urban Atlanta on August 20, 2002.

density of the evaporated mass for 100 nm particles ranged from 1.25 g/cm^3 to 1.45 g/cm^3. Lower density species such as n-alkanes in lubricating oil have densities in the range of 1.0 g/cm^3, while densities of secondary organics (Lim and Turpin 2002; Ziemann 2002), and high molecular weight oligomeric materials (Kalberer et al. 2004) are in the range 1.0–1.6 g/cm^3. These species would volatilize at temperatures below 300°C. These measurements show that the VTDMA-APM method is a promising approach for measuring changes in aerosol properties as they evaporate, and these are the first such results to be reported. More systematic studies of this type in a variety of locations are needed to understand how properties of volatilized mass vary with location, particle size, and particle composition.

We also used the VTDMA-ATOFMS to measure the chemical compositions of 300 nm "more volatile" and "less volatile" atmospheric particles separated at a conditioner temperature of 150°C by the VTDMA. Illustrative results of these exploratory studies are shown in Figure 9, which shows averaged spectra of

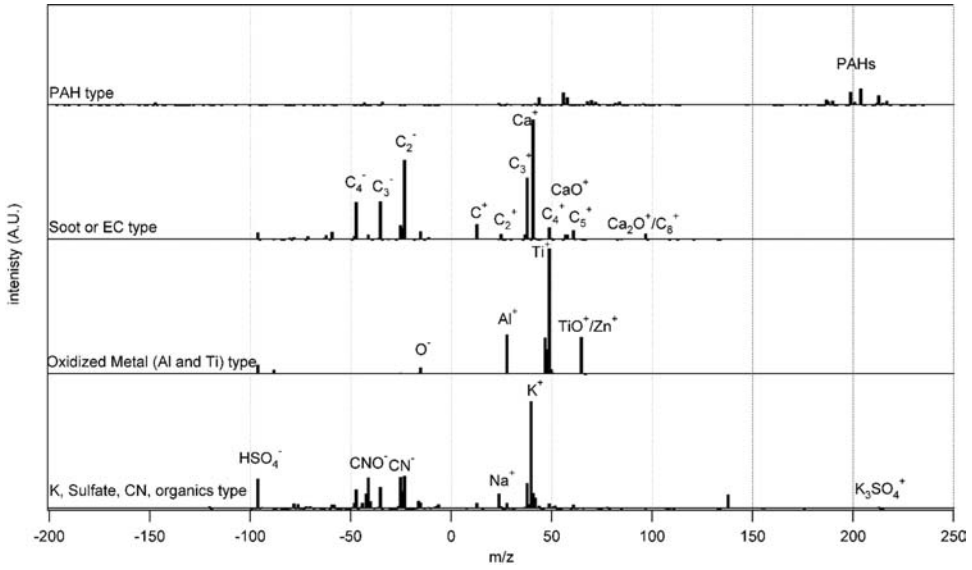

FIG. 10. VTDMA-ATOFMS measurements of average mass spectra for the four types of "less volatile" 300 nm mobility diameter particles in urban Atlanta on August 20, 2002: (a) "Soot or EC" (14%), (b) "PAH" (22%), (c) "K, sulfate, CN compounds, and organics" (57%), and (d) "oxidized metals" (7%).

more and less volatile particles in Atlanta. There are clear qualitative differences in these spectra. Elemental carbon, potassium, oxidized organics, and organic nitrates are more abundant in the "less volatile" particles, while ammonium, ammonium sulfate, sulfate, phosphate, and phosphoric acid are more abundant in the "more volatile" particles. As was mentioned above, VTDMA-APM measurements showed that the effective density of the evaporated mass from the "more volatile" 300 nm particles was close to the density of ammonium sulfate, which is consistent with these chemical composition data. Based on ATOFMS measurements, we grouped the "less volatile" particles into several distinct particle types: "Soot or EC," "PAH," "K, sulfate, CN compounds and organics," and "oxidized metals" with dominantly Al and Ti as shown in Figure 10. Observations from the Prather group were used to distinguish between EC and OC (Spencer and Prather 2006). The average fractions of these particle types were: Soot or EC (14%), PAH (21%), K, sulfate, CN compounds and organics (57%), and oxidized metals (7%).

CONCLUSIONS

Measurements of mobility size in tandem with other properties enable a far more detailed characterization of aerosol physical and chemical properties than can be achieved with one measurement alone. Indeed, such techniques are moving aerosol measurement towards the ideal envisioned by Friedlander nearly four decades ago, when he discussed the need for instrumentation to measure an aerosol's composition probability density function (Friedlander 1970, 1971). Such measurements can establish relationships between different measurements of size, can provide information on particle properties such as shape, density, vapor pressure and reactivity, and can quantify variabilities in properties among particles of a given mobility size. Such measurements also enable quantitative investigations into the effects on properties of aerosol processing by chemical reactions, vapor condensation or evaporation. It is likely that many additional tandem measurement methods will be developed in the future.

REFERENCES

Abbatt, J. P. D., Broekhuizen, K., and Kumal, P. P. (2005). Cloud Condensation Nucleus Activity of Internally Mixed Ammonium Sulfate/Organic Acid Aerosol Particles, *Atmos. Environ.* 39:4767–4778.

Barone, T. L., Lall, A. A., Zhu, Y. F., Yu, R. C., and Friedlander, S. K. (2006). Inertial Deposition of Nanoparticle Chain Aggregates: Theory and Comparison with Impactor Data for Ultrafine Atmospheric Aerosols, *J. Nanoparticle Res.* 8:669–680.

Bilde, M., and Svenningsson, B. (2004). CCN Activation of Slightly Soluble Organics: The Importance of Small Amounts of Inorganic Salt and Particle Phase, *Tellus Series B—Chem. Phys. Meteorol.* 56:128–134.

Canagaratna, M. R., Jayne, J. T., Onasch, T. B., Williams, L. R., Trimborn, A. M., Northway, M. J., Kolb, C. E., Worsnop, D. R., Jimenez, J., L., Alfarra, M. R., Zhang, Q., Drewnick, F., and Davidovits, P. (2007). Chemical and Microphysical Characterization of Ambient Aerosols with the Aerosol Mass Spectrometer, *Mass Spec. Reviews* 26:185–222.

Chan, P., and Dahneke, B. (1981). Free-molecule Drag on Straight Chains of Uniform Spheres, *J. Appl. Phys.* 52:3106–3110.

Chen, D. R., Pui, D. Y. H., Hummes, D., Fissan, H., Quant, F. R., and Sem, G. J. (1998). Design and Evaluation of a Nanometer Aerosol Differential Mobility Analyzer (Nano-DMA), *J. Aerosol Sci.* 29:497–509.

Cho, K., Hogan, C. J., and Biswas, P. (2007). Study of the Mobility, Surface Area, and Sintering Behavior of Agglomerates in the Transition Regime by Tandem Differential Mobility Analysis, *J. Nanoparticle Res.* 9:1003–1012.

Clemmer, D. E., Hudgins, R. R., and Jarrold, M. F. (1995). Naked Protein Conformations: Cytochrome c in the Gas Phase, *J. Am. Chem. Soc.* 117:10141–10142.

Cooke, D. D., and Kerker, M. (1975). Response Calculations for Light Scattering Aerosol Particle Counters, *Appl. Opt.* 14:734–739.

Corrigan, C. E., and Novakov, T. (1999). Cloud Condensation Nucleus Activity of Organic Compounds: A Laboratory Study, *Atmos. Environ.* 33:2661–2668.

Covert, D. S., Heintzenberg, J., and Hansson, H. C. (1990). Electro–Optical Detection of External Mixtures in Aerosols, *Aerosol Sci. Technol.* 12:446–456.

Cruz, C., and Pandis, S. N. (1997). A Study of the Ability of Pure Secondary Organic Aerosol to Act as Cloud Condensation Nuclei, *Atmos. Environ.* 31:2205–2214.

Cruz, C. N., and Pandis, S. N. (1998). The Effect of Organic Coatings on the Cloud Condensation Nuclei Activation of Inorganic Atmospheric Aerosol, *J. Geophys. Res.—Atmospheres* 103:13111–13123.

Cubison, M. J., Coe, H., and Gysel, M. (2005). A Modified Hygroscopic Tandem DMA and a Data Retrieval Method Based on Optimal Estimation, *J. Aerosol Sci.* 36:846–865.

de la Mora, J. F., de Juan, L., Liedtke, K., and Schmidt-Ott, A. (2003). Mass and Size Determination of Nanometer Particles by Means of Mobility Analysis and Focused Impaction, *J. Aerosol Sci.* 34:79–98.

DeCarlo, P. F., Slowik, J. G., Worsnop, D. R., Davidovits, P., and Jimenez, J. L. (2005). Particle Morphology and Density Characterization by Combined Mobility and Aerodynamic Diameter Measurements. Part 1: Theory, *Aerosol Sci. Technol.* 38:1185–1205.

Delene, D. J., and Deshler, T. (2000). Calibration of a Photometric Cloud Condensation Nucleus Counter Designed for Deployment on a Balloon Package, *J. Atmos. Oceanic Technol.* 17:459–467.

Dick, W. D., and McMurry, P. H. (2007). Mulitangle Light-Scattering Measurements of Refractive Index of Submicron Atmospheric Particles (doi:10.1080/02786820701272012), *Aerosol Sci. Technol.* 41:549–569.

Dick, W. D., Saxena, P., and McMurry, P. H. (2000). Estimation of Water Uptake by Organic Compounds in Submicron Aerosols Measured During the Southeastern Aerosol and Visibility Study, *J. Geophys. Res.—Atmospheres* 105:1471–1479.

Dick, W. D., Ziemann, P. J., Huang, P. F., and McMurry, P. H. (1998). Optical Shape Fraction Measurements of Submicrometre Laboratory and Atmospheric Aerosols, *Meas. Sci. Technol.* 9:183–196.

Dockery, D. W., and Pope, C. A. (1994). Acute Respiratory Effects of Particulate Air Pollution, *Ann. Rev. Public Health* 15:107–132.

Ehara, K., Hagwood, C., and Coakley, K. J. (1996). Novel Method to Classify Aerosol Particles According to Their Mass-to-Charge Ratio: Aerosol Particle Mass Analyser, *J. Aerosol Sci.* 27:217–234.

Eiceman, G. A., and Karpas, Z. (2005). *Ion Mobility Spectrometry*. Taylor & Francis, Boca Raton, FL.

Emery, M. (2005). Theoretical Analysis of Data from DMA–APM System, in *Mechanical Engineering*, University of Minnesota, Minneapolis, MN, 63.

Fernández de la Mora, J. F., de Juan, L., Eichler, T., and Rosell, J. (1998). Differential Mobility Analysis of Molecular Ions and Nanometer Particles, *Trends in Anal. Chem.* 17:328–338.

Friedlander, S. K. (1970). The Characterization of Aerosols Distributed With Respect to Size and Chemical Composition, *J. Aerosol Sci.* 1:295–307.

Friedlander, S. K. (1971). The Characterization of Aerosols Distributed with respect to Size and Chemical Composition—II, *Aerosol Sci.* 2:331–340.

Gard, E., Mayer, J., Morrical, B. D., Dienes, T., Fergenson, D. P., and Prather, K. A. (1997). Real–Time Analysis of Individual Atmospheric Aerosol Particles: Design and Performance of a Portable ATOFMS, *Anal. Chem.* 69:4083–4091.

Geller, M., Biswas, S., and Sioutas, C. (2006). Determination of Particle Effective Density in Urban Environments With a Differential Mobility Analyzer and Aerosol Particle Mass Analyzer, *Aerosol Sci. Technol.* 40:709–723.

Gupta, A., Tang, D., and McMurry, P. H. (1995). Growth of Monodisperse, Submicron Aerosol Particles Exposed to SO_2, H_2O_2, and NH_3, *J. Atmos. Chem.* 20:117–139.

Heintzenberg, J., Okada, K., and Lui, B. P. (2002). Distribution of Optical Properties Among Atmospheric Submicrometer Particles of Given Electrical Mobilities, *J. Geophys. Res. Atmospheres* 107:4107–4115.

Heintzenberg, J., Okada, K., Trautmann, T., and Hoffmann, P. (2004). Modeling of the Signals of an Optical Particle Counter for Real Nonspherical Particles, *Appl. Opt.* 43:5893–5900.

Hering, S., and McMurry, P. H. (1991). Optical Counter Response to Monodisperse Atmospheric Aerosols, *Atmos. Environ.* 25A:463–468.

Hering, S. V., Flagan, R. C., and Friedlander, S. K. (1977). Design and Evaluation of a New Low Pressure Impactor I, *Environ. Sci. Technol.* 12:667–673.

Hering, S. V., and Friedlander, S. K. (1979). Design and Evaluation of a New Low-Pressure Impactor. 2, *Environ. Sci. Technol.* 13:184–188.

Hering, S. V., and Stolzenburg, M. R. (1995). On-Line Determination of Particle Size and Density in the Nanometer Size Range, *Aerosol Sci. Technol.* 23:155–173.

Heyder, J., and Gebhart, J. (1979). Optimization of Response Functions of Light Scattering Instruments for Size Evaluation of Aerosol Particles, *Appl. Opt.* 18:705–711.

Hinds, W. C. (1999), *Aerosol Technology: Properties, Behavior, and Measurement of Airborne Particles*. John Wiley & Sons, Inc., New York.

Holm, J., and Roberts, J. T. (2007). Thermal Oxidation of 6 nm Aerosolized Silicon Nanoparticles: Size and Surface Chemistry Changes, *Langmuir* 23:11217–11224.

Hudson, J. G. (1989). An Instantaneous CCN Spectrometer, *J. Atmos. Oceanic Technol.* 6:1055–1065.

IPCC (2007), *Climate Change 2007: IPCC Fourth Assessment Report (AR4)*. Cambridge University Press.

Jung, H., Kittelson, D. B., and Zachariah, M. R. (2004). Kinetics and Visualization of Soot Oxidation Using Transmission Electron Microscopy, *Combustion and Flame* 136:445–456.

Kalberer, M., Paulsen, D., Sax, M., Seteinbacher, M., Dommen, J., Prevot, A. S. H., Fisseha, R., Weingartner, E., Frankevich, V., Zenobi, R., and Baltensperger, U. (2004). Identification of Polymers as Major Components of Atmospheric Organic Aerosols, *Science* 303:1659–1665.

Kasper, G. (1982). Dynamics and Measurement of Smokes. I. Size Characterization of Nonspherical Particles, *Aerosol Sci. Technol.* 1:187–199.

Kaufman, S. L. (1998). Analysis of Biomolecules Using Electrospray and Nanoparticle Methods: The Gas-Phase Electrophoretic Mobility Molecular Analyzer (GEMMA), *J. Aerosol Sci.* 29:537–552.

Kelly, W. P., and McMurry, P. H. (1992). Measurement of Particle Density by Inertial Classification of Differential Mobility Analyzer–Generated Monodisperse Aerosols, *Aerosol Sci. Technol.* 17:199–212.

Kim, S. H., Mulholland, G. W., and Zachariah, M. R. (2007). Understanding Ion-Mobility and Transport Properties of Aerosol Nanowires, *J. Aerosol Sci.* 38:823–842.

Kim, S. H., and Zachariah, M. R. (2005). In-Flight Size Classification of Carbon Nanotubes by Gas-Phase Electrophoresis, *NanoTechnology* 16.

Kim, S. H., and Zachariah, M. R. (2006). In-Flight Kinetic Measurements of the Aerosol Growth of Carbon Nanotubes by Electrical Mobility Classification, *J. Phys. Chem. B* 110:4555–4562.

Knutson, E. O., and Whitby, K. T. (1975). Aerosol Classification by Electric Mobility: Apparatus, Theory, and Application, *J. Aerosol Sci.* 6:443–451.

Kousaka, Y., Endo, Y., Ichitsubo, H., and Alonso, M. (1996). Orientation-Specific Dynamic Shape Factors for Doublets and Triplets of Spheres in the Transition Regime, *Aerosol Sci. Technol.* 24:36–44.

Lall, A. A., and Friedlander, S. K. (2006). On-Line Measurement of Ultrafine Aggregate Surface Area and Volume Distributions by Electrical Mobility Analysis: 1. Theoretical Analysis, *J. Aerosol Sci.* 37:260–271.

Lall, A. A., Rong, W., Mädler, L., and Friedlander, S. K. (2008). Nanoparticle Aggregate Volume Determination by Electrical Mobility Analysis: Test of Idealized Aggregate Theory Using Aerosol Particle Mass Analyzer Measurements, *J. Aerosol Sci.* in press.

Lall, A. A., Seipenbusch, M., Rong, W. Z., and Friedlander, S. K. (2006). On-Line Measurement of Ultrafine Aggregate Surface Area and Volume Distributions by Electrical Mobility Analysis: II. Comparison of Measurements and Theory, *J. Aerosol Sci.* 37:272–282.

Li, Z., and Wang, H. (2003a). Drag Force, Diffusion Coefficient, and Electrical Mobility of Small Particles. I. Theory Applicable to the Free-Molecule Regime, *Phys. Rev. E* 68:061206–061201 to 061206–061209.

Li, Z., and Wang, H. (2003b). Drag Force, Diffusion Coefficient, and Electrical Mobility of Small Particles. II. Application, *Phys. Rev. E* 68:061207–061201 to 061207–061213.

Liao, Y. C., Nienow, A. M., and Roberts, J. T. (2006). Surface Chemistry of Aerosolized Nanoparticles: Thermal Oxidation of Silicon, *J. Phys. Chem. B* 110:6190–6197.

Liao, Y. C., and Roberts, J. T. (2006). Self–Assembly of Organic Monolayers on Aerosolized Silicon Nanoparticles, *Journal of the American Chemical Society* 128:9061–9065.

Lilienfeld, P. (1985). Rotational Electrodynamics of Airborne Fibers, *J. Aerosol Sci.* 16:315–322.

Lim, H. J., and Turpin, B. J. (2002). Origins of Primary and Secondary Organic Aerosol in Atlanta: Results of Time-Resolved Measurements During the Atlanta Supersite Experiment, *Environ. Sci. Technol.* 36:4489–4496.

Liu, B. Y. H., and Pui , D. Y. H. (1974). A Submicron Aerosol Standard and the Primary, Absolute Calibration of the Condensation Nuclei Counter, *J. Colloid Interface Sci.* 47:155–171.

Liu, B. Y. H., Pui, D. Y. H., Whitby, K. T., Kittelson, D. B., Kousaka, Y., and McKenzie, R. L. (1978). The Aerosol Mobility Chromatograph: A New Detector for Sulfuric Acid Aerosols, *Atmos. Environ.* 12:99–104.

Liu, Y. G., and Daum, P. H. (2000). The Effect of Refractive Index on Size Distributions and Light Scattering Coefficients Derived from Optical Particle Counters, *J. Aerosol Sci.* 31:945–957.

Maricq, M. M., and Xu, N. (2004). The Effective Density and Fractal Dimension of Soot Particles from Premixed Flames and Motor Vehicle Exhaust, *J. Aerosol Sci.* 35:1251–1274.

Marple, V. A., Rubow, K. L., and Behm, S. M. (1991). A Microorifice Uniform Deposit Impactor (MOUDI): Description, Calibration, and Use, *Aerosol Sci. Technol.* 14:434–446.

McMurry, P. H. (2000). A Review of Atmospheric Aerosol Measurements, *Atmos. Environ.* 34:1959–1999.

McMurry, P. H., and Eisele, F. L. (2005). Preface to Topical Collection on New Particle Formation in Atlanta—Art. no. D22S01, *J. Geophys. Res.—Atmospheres* 110:S2201.

McMurry, P. H., Litchy, M., Huang, P. F., Cai, X. P., Turpin, B. J., Dick, W. D., and Hanson, A. (1996). Elemental Composition and Morphology of Individual Particles Separated by Size and Hygroscopicity with the TDMA, *Atmos. Environ.* 30:101–108.

McMurry, P. H., Shepherd, M., and Vickery, J., eds. (2004), *Particulate Matter Science for Policy Makers: A NARSTO Assessment*. Cambridge University Press.

McMurry, P. H., and Stolzenburg, M. R. (1989). On the Sensitivity of Particle Size to Relative Humidity for Los Angeles Aerosols, *Atmos. Environ.* 23:497–507.

McMurry, P. H., Takano, H., and Anderson, G. R. (1983). A Study of the Ammonia Gas–Sulfuric Acid Aerosol Reaction Rate, *Environ. Sci. Technol.* 17:347–352.

McMurry, P. H., Wang, X., Park, K., and Ehara, K. (2002). The Relationship between Mass and Mobility for Atmospheric Particles: A New Technique for Measuring Particle Density, *Aerosol Sci. Technol.* 36:227–238.

Müller, R., Laschober, C., Szymanski, W. W., and Allmaier, G. (2007). Determination of Molecular Weight, Particle Size, and Density of High

Number Generation PAMAM Dendrimers using MALDI-TOF-MS and nES-GEMMA, *Macromolecules* 40:5599–5605.

Nakaso, K., Shimada, M., Okuyama, K., and Deppert, K. (2002). Evaluation of the Change in the Morphology of Gold Nanoparticles During Sintering, *J. Aerosol Sci.* 33:1061–1074.

Naoe, H., and Okada, K. (2001). Mixing Properties of Submicrometer Aerosol Particles in the Urban Atmosphere—With Regard to Soot Particles, *Atmos. Environ.* 35:5765–5772.

Nash, D. G., Baer, T., and Johnston, M. V. (2006). Aerosol Mass Spectrometry: A Historical Review of a Quarter Century of the Chemical Analysis of Aerosols, *Mass Spec. Reviews* 198:248–274.

Neville, M., McCarthy, J. F., and Sarofim, A. F. (1983). Size Fractionation of Submicrometer Coal Combustion Aerosol for Chemical Analysis, *Atmos. Environ.* 17:2599–2604.

Noble, C. A., and Prather, K. A. (2000). Real-Time Single Particle Mass Spectrometry: A Historical Review of a Quarter Century of the Chemical Analysis of Aerosols [Review], *Mass Spec. Reviews* 19:248–274.

NRC. (1993), *Protecting Visibility in National Parks and Wilderness Areas*. National Academy Press, Washington, D.C.

Oberdörster, G. (2000). Toxicology of Ultrafine Particles: *In Vivo* Studies, *Philosophical Transactions of the Royal Society of London* 358:22719–22740.

Okada, K., and Heintzenberg, J. (2003). Size Distribution, State of Mixture and Morphology of Urban Aerosol Particles at Given Electrical Mobilities, *J. Aerosol Sci.* 34:1539–1553.

Olfert, J. S., Symnonds, J. P. R., and Collings, N. (2007). The Effective Density and Fractal Dimension of Particles Emitted from a Light-Duty Diesel Vehicle with a Diesel Oxidation Catalyst, *J. Aerosol Sci.* 38:69–82.

Orsini, D. A., Wiedensohler, A., Stratmann, F., and Covert, D. S. (1999). A New Volatility Tandem Differential Mobility Analyzer to Measure the Volatile Sulfuric Acid Aerosol Fraction, *Journal of Atmospheric & Oceanic Technology* 16:760–772.

Pandis, S., Solomon, P. A., and Scheffe, R. (2005). Preface to Special Section on Particulate Matter Supersites—Art. No. D07S01, *J. Geophys. Res.—Atmospheres* 110:S701.

Park, K., Cao, F., Kittelson, D. B., and McMurry, P. H. (2003a). Relationship between Particle Mass and Mobility for Diesel Exhaust Particles, *Environ. Sci. Technol.* 37:577–583.

Park, K., Kittelson, D. B., and McMurry, P. H. (2003b). A Closure Study of Aerosol Mass Concentration Measurements: Comparison of Values Obtained with Filters and by Direct Measurements of Mass Distributions, *Atmos. Environ.* 37:1223–1230.

Park, K., Kittelson, D. B., and McMurry, P. H. (2004a). Measurement of Inherent Material Density of Nanoparticle Agglomerates, *J. Nanoparticle Res.* 6:267–272.

Park, K., Kittelson, D. B., and McMurry, P. H. (2004b). Structural Properties of Diesel Exhaust Particles Measured by Transmission Electron Microscopy (TEM): Relationships to Particle Mass and Mobility, *Aerosol Sci. Technol.* 38:881–889.

Park, K., Kittelson, D. B., Zachariah, M. R., and McMurry, P. H. (2004d). Measurement of Inherent Material Density of Nanoparticle Agglomerates, *J. Nanoparticle Res.* 6:267–272.

Peters, A., Wichmann, H. E., Tuch, T., Heingrich, J., and Heyder, J. (1997). Respioratory Effects are Associated with the Number of Ultrafine Particles, *Am. J. Respir. Crit. Care Med.* 155:1376–1383.

Petters, M. D., Prenni, A. J., Kreidenweis, S. M., and DeMott, P. J. (2007). On Measuring the Critical Diameter of Cloud Condensation Nuclei Using Mobility Selected Aerosol, *Aerosol Sci. Technol.* 41:907–913.

Philippin, S., Wiedensohler, A., and Stratmann, F. (2004). Measurements of Non-Volatile Fractions of Pollution Aerosols with an Eight-Tube Volatility Tandem Differential Mobility Analyzer (VTDMA-8), *J. Aerosol Sci.* 35:185–203.

Rader, D. J., and McMurry, P. H. (1986). Application of the Tandem Differential Mobility Analyzer to Studies of Droplet Growth or Evaporation, *J. Aerosol Sci.* 17:771–787.

Rader, D. J., McMurry, P. H., and Smith, S. (1987). Evaporation Rates of Monodisperse Organic Aerosols in the 0.02 to 0.2 μm Diameter Range, *Aerosol Sci. Technol.* 6:247–260.

Riipinen, I., Koponen, I. K., Frank, G. P., Hyvaerinen, A. P., Vanhanen, J., Lihavainen, H., Lehtinen, K. E. J., Bilde, M., and Kulmala, M. (2007). Adipic and Malonic Acid Aqueous Solutions: Surface Tensions and Saturation Vapor Pressures, *J. Phys. Chem. A* 111:12995–13002.

Roberts, G. C., and Nenes, A. (2005). A Continuous-Flow Streamwise Thermal-Gradient CCN Chamber for Atmospheric Measurements, *Aerosol Sci. Technol.* 39:206–221.

Rogak, S. N., and Flagan, R. C. (1993). The Mobility and Structure of Aerosol Agglomerates, *Aerosol Sci. Technol.* 18:25–47.

Sachweh, B. A., Dick, W. D., and McMurry, P. H. (1995). Distinguishing between Spherical and Nonspherical Particles by Measuring the Variability in Azimuthal Light Scattering, *Aerosol Sci. Technol.* 23:373–391.

Sakurai, H., Park, K., McMurry, P. H., Zarling, D. D., Kittelson, D. B., and Ziemann, P. J. (2003a). Size-Dependent Mixing Characteristics of Volatile and Nonvolatile Components in Diesel Exhaust Aerosols, *Environ. Sci. Technol.* 37:5487–5495.

Sakurai, H., Tobias, H. J., Park, K., Zarling, D., Docherty, S., Kittelson, D. B., McMurry, P. H., and Ziemann, P. J. (2003b). On-Line Measurements of Diesel Nanoparticle Composition and Volatility, *Atmos. Environ.* 37:1199–1210.

Saxena, P., and Hildemann, L. M. (1996). Water-Soluble Organics in Atmospheric Particles: A Critical Review of the Literature and Application of Thermodynamics to Identify Candidate Compounds, *J. Atmos. Chem.* 24:57–109.

Saxena, P., and Hildemann, L. M. (1997). Water Absorption by Organics: Survey of Laboratory Evidence and Evaluation of UNIFAC for Estimating Water Activity, *Environ. Sci. Technol.* 31:3318–3324.

Sioutas, C., Pandis, S. N., Allen, D. T., and Solomon, P. A. (2004). Special issue of Atmospheric Environment on Findings from EPA's Particulate Matter Supersites Program—Preface, *Atmos. Environ.* 38:3101–3106.

Skillas, G., Kunzel, S., Burtscher, H., Baltensperger, U., and Siegmann, K. (1998). High Fractal-Like Dimension of Diesel Soot Agglomerates, *J. Aerosol Sci.* 29:411–419.

Slowik, J. G., Stainken, K., Davidovits, P., Williams, L. R., Jayne, J. T., Kolb, C. E., Worsnop, D. R., Rudich, Y., DeCarlo, P. F., and Jimenez, J. L. (2004). Particle Morphology and Density Characterization by Combined Mobility and Aerodynamic Diameter Measurements. Part 2: Application to Combustion-Generated Soot Aerosols as a Function of Fuel Equivalence Ratio, *Aerosol Sci. Technol.* 38:1206–1222.

Smith, J. N., Dunn, M. J., VanReken, T. M., Iida, K., Stolzenburg, M. R., McMurry, P. H., and Huey, L. G. (2008). The Chemical Composition of Atmospheric Nanoparticles Formed from Nucleation in Tecamac, Mexico: Evidence for an Important Role for Organic Species in Nanoparticle Growth, *Geophys. Res. Lett.* 35:L04808, doi:04810.01029/02007GL032523.

Smith, J. N., Moore, K. F., Eisele, F. L., Voisin, D., Ghimire, A. K., Sakurai, H., and McMurry, P. H. (2005). Chemical Composition of Atmospheric Nanoparticles During Nucleation Events in Atlanta—Art. No. D22S03, *J. Geophys. Res.—Atmospheres* 110:S2203.

Smith, J. N., Moore, K. F., McMurry, P. H., and Eisele, F. L. (2004). Atmospheric Measurements of Sub–20 nm Diameter Particle Chemical Composition by Thermal Desorption Chemical Ionization Mass Spectrometry, *Aerosol Sci. Technol.* 38:100–110.

Sorooshian, A., Hersey, S., Brechtel, F. J., Corless, A., Flagan, R. C., and Seinfeld, J. H. (2008). Rapid, Size-Resolved Aerosol Hygroscopic Growth Measurements: Differential Aerosol Sizing and Hygroscopicity Spectrometer Probe (DASH-SP), *Aerosol Sci. Technol.* in press.

Spencer, M. T., and Prather, K. A. (2006). Using ATOFMS to Determine OC/EC Mass Fractions in Particles, *Aerosol Sci. Technol.*40:585–594.

Stanier, C. O., and Solomon, P. A. (2006). Preface to Special Section on Particulate Matter Supersites Program and Related Studies, *J. Geophys. Res.—Atmospheres* 111:D10S01

Stein, S. W., Turpin, B. J., Cai, X. P., Huang, C. P. F., and McMurry, P. H. (1994). Measurements of Relative Humidity–Dependent Bounce and Density for Atmospheric Particles Using the DMA-Impactor Technique, *Atmos. Environ.* 28:1739–1746.

Stolzenburg, M. R., and McMurry, P. H. (1988). TDMAFIT User's Manual, Particle Technology Laboratory, Department of Mechanical Engineering, University of Minnesota, Minneapolis, MN.

Swietlicki, E., Hansson, H.-C., Hämeri, K., Svenningsson, B., Massling, A., McFiggans, G., McMurry, P. H., Petäjä, T., Tunved, P., Gysel, M., Topping, D., Weingartner, E., Baltensperger, U., Rissler, J., Wiedensohler, A., and Kulmala, M. (2008). Hygroscopic Properties of Sub-Micrometer Atmospheric Aerosol Particles Measured with H-TDMA Instruments in Various Environments—A Review, *Tellus Series B—Chemical and Physical Meteorology* doi: 10.1111/j.1600–0889.2008.00350.x.

Szymanski, W. W., and Liu, B. Y. H. (1986). On the Sizing Accuracy of Laser Optical Particle Counters, *Part. Charact.* 3:1–7.

Tammet, H. (1995). Size and Mobility of Nanometer Particles, Clusters and Ions, *J. Aerosol Sci.* 26:459–475.

Tao, Y., and McMurry, P. H. (1989). Vapor Pressures and Surface Free Energies of C14 to C18 Monocarboxylic Acids and C5 and C6 Dicarboxylic Acids, *Environ. Sci. Technol.* 23:1519–1523.

Ude, S., and de la Mora, J. F. (2003). Hypersonic Impaction with Molecular Mass Standards, *J. Aerosol Sci.* 34:1245–1266.

Ude, S., de la Mora, J. F., Alexander, J. N., and Saucy, D. A. (2006). Aerosol Size Standards in the Nanometer Size Range II. Narrow Size Distributions of Polystyrene 3–11 nm in Diameter, *J. Colloid & Interface Sci.* 293:384–393.

Ude, S., and Mora, F. D. L. (2005). Molecular Monodisperse Mobility and Mass Standards from Electrosprays of Tetra-Alkyl Amonium Halides, *J. Aerosol Sci.* 36:1224–1237.

Villani, P., Picard, D., Marchand, N., and Laj, P. (2007). Design and Validation of a 6-Volatility Tandem Differential Mobility Analyzer (VTDMA), *Aerosol Sci. Technol.*41:898–906.

Voisin, D., Smith, J. N., Sakurai, H., McMurry, P. H., and Eisele, F. L. (2003). Thermal Desorption Chemical Ionization Mass Spectrometer for Ultrafine Particle Chemical Composition, *Aerosol Sci. Technol.* 37:471–475.

von Helden, G., Hsu, M.–T., Kemper, P. R., and Bowers, M. T. (1991). Structures of Carbon Cluster Ions from 3 to 60 Atoms: Linears to Rings to Fullerenes, *J. Chem. Phys.* 95:3835–3837.

Wang, X. (2002). Optical Particle Counter (OPC) Measurements and Pulse Height Analysis (PHA) Data Inversion, in *Mechanical Engineering*, University of Minnesota, Minneapolis, MN, 151.

Weingartner, E., Burtscher, H., and Baltensperger, U. (1997). Hygroscopic Properties of Carbon and Diesel Soot Particles, *Atmos. Environ.* 31:2311–2327.

Wyatt, P. J., Schehrer, K. L., Philips, S. D., Jackson, C., Chang, Y.-J., Parker, R. G., Phillips, D. T., and Bottiger, J. R. (1988). Aerosol Particle Analyzer, *Appl. Opt.* 27:217–221.

Wyttenbach, T., and Bowers, M. T. (2007). Intermolecular Interactions in Biomolecular Systems Examined by Mass Spectrometry. *Ann. Rev. Phys. Chem.* 58:511–533.

Zelenyuk, A., and Imre, D. (200). On the Effect of Particle Alignment in the DMA, *Aerosol Sci. Technol.* 41:112–124.

Zhang, B., Liao, Y. C., Girshick, S. L., and Roberts, J. T. (2008a). Growth of Coatings on Nanoparticles by Photoinduced Chemical Vapor Deposition, *J. Nanoparticle Res.* 10:173–178.

Zhang, R., Khalizov, A., Pagels, J., Zhang, D., Xue, H., and McMurry, P. H. (2008b). Remarkable Variability in Morphology, Hygroscopicity and Optical Properties of Soot Aerosols during Atmospheric Processing, *Proc. National Acad. Sci.* in press.

Ziemann, P. J. (2002). Evidence for Low-Volatility Diacyl Peroxides as a Nucleating Agent and Major Component of Aerosol Formed from Reactions of O3 with Cyclohexene and Homologous Compounds, *J. Phys. Chem. A* 106:4390–4402.